Additivity of the Excess Energy Dissipation Rate in a Dynamically Self-Assembled System

ARTICLE *in* THE JOURNAL OF PHYSICAL CHEMISTRY B · JUNE 2009

Impact Factor: 3.3 · DOI: 10.1021/jp811473q · Source: PubMed

3 AUTHORS, INCLUDING:

Konstantin Tretiakov
Institute of Molecular Physics, Polish Acad…
36 PUBLICATIONS **518** CITATIONS
SEE PROFILE

Kyle J M Bishop
Pennsylvania State University
80 PUBLICATIONS **2,988** CITATIONS
SEE PROFILE

Additivity of the Excess Energy Dissipation Rate in a Dynamically Self-Assembled System

Konstantin V. Tretiakov,[†,§] Kyle J. M. Bishop,*[,†] and Bartosz A. Grzybowski*[,†,‡]

Department of Chemical and Biological Engineering and Department of Chemistry, Northwestern University, 2145 Sheridan Road, Evanston, Illinois 60208, and Institute of Molecular Physics, Polish Academy of Sciences, Smoluchowskiego 17/19, 60-179 Poznań, Poland

Received: December 29, 2008; Revised Manuscript Received: March 5, 2009

Despite its prevalence in biological systems and its promise as a route to adaptive and/or self-healing materials, dynamic self-assembly (DySA) far from thermodynamic equilibrium remains poorly understood. In this context, it is desirable to develop general thermodynamic relations describing the steady-state configurations of such dissipative assemblies. Here, numerical simulations and analytical methods are used to calculate the viscous energy dissipation rates in a prototypical, magnetohydrodynamic DySA system. In addition to the well-established criteria of mechanical equilibrium, it is shown that the naturally forming steady-state configurations/flows are characterized by a fundamentally different relation based on the viscous energy dissipation. Specifically, the total dissipation of the *n*-particle system may be expressed as a sum of pairwise "interactions" derived from the analogous two-particle system. This dissipation additivity holds despite the presence of many-body forces/torques between the particles and may prove useful in estimating the viscosities of colloidal suspensions.

1. Introduction

Self-assembly (SA)[1,2] is a process in which discrete components organize spontaneously, that is, without any human intervention, into ordered and/or functional superstructures,[1] and is an elegant alternative to "top-down" fabrication methods. Examples of widely used and technologically promising SA systems include self-assembled monolayers,[3,4] liquid crystals,[5,6] metal−organic frameworks,[7] micelles,[8] nanostructured materials,[9] photonic crystals,[10] self-building electric circuits,[11] and polymer sacs/membranes.[12] The vast majority of these and other man-made SA systems are stable structures that correspond to the minima of appropriate thermodynamic potentials (Figure 1, Top). In sharp contrast, many biological examples of SA are nonequilibrium structures that require constant supply of energy which they continuously dissipate in order to maintain the organized state (Figure 1, Bottom). As we have argued in detail elsewhere,[2] these dissipative or "dynamic" SA (DySA) systems have the capacity to exhibit adaptability, self-healing, and even self-replication, and can therefore be considered as candidates for the "smart" materials of the future.

From a theoretical perspective, DySA structures belong to a broad class of nonequilibrium (NE) steady-state systems (or "dissipative structures"[13]), in which the production of entropy (i.e., dissipation of useful energy) directs the emergence of order (cf. Figure 1b). Such dissipative structures can be understood qualitatively as nature's "optimal" solutions for the efficient degradation of thermodynamic gradients via dissipative processes. A generalized quantitative description, however, remains lacking. For small displacements from equilibrium,[14] it is well established that nonequilibrium systems evolve to steady-state configurations that minimize entropy production (MEP) subject to the externally imposed NE constraints (e.g., an imposed temperature gradient).[15] Beyond this so-called linear regime of NE thermodynamics, no general variational principle exists, and one must typically rely on specific models to describe a system's dynamics.

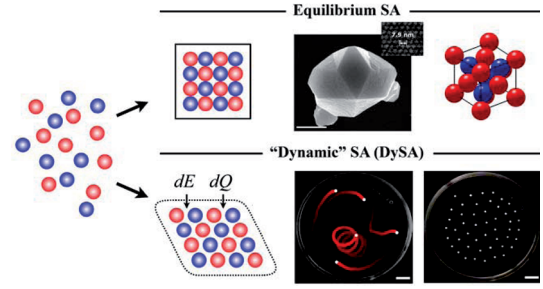

Figure 1. (Top) In equilibrium self-assembly, components organize to minimize an appropriate thermodynamic potential. The resulting assembly is closed from its surroundings in the sense that are no systematic flows of mass, momentum, or energy into or out of the system. Examples include the electrostatic self-assembly of the charged nanoparticles into diamond-like superlattices with ZnS crystal structure (top right).[9] (Bottom) In nonequilibrium or "dynamic" self-assembly (DySA), the ordered structures that form are maintained only through a constant supply of energy, d*E*, which is subsequently dissipated as heat, d*Q*, through the components' interactions with each other and with their environment. Examples include DySA via dynamic surface tension,[31] in which hydrogel particles doped with camphor and floating at a water−air interface move about spontaneously and ultimately organize into open lattice assemblies due to repulsive interactions caused by the Marangoni-type flows. Scale bars = 5 mm.

Unfortunately, there are currently very few man-made systems that would be complex enough to exhibit DySA yet simple enough to quantify the relationship(s) between the mode(s) of system's organization and energy dissipation. In this article, we study such a relationship for a model DySA system of magnetic particles spinning under the influence of an external magnetic field at a liquid−air interface and interacting via vortex−vortex interactions (Figure 2). In a series of previous papers, we[16−19]

* To whom correspondence should be addressed. E-mail: grzybor@northwestern.edu (B.A.G.); kjmbishop@u.northwestern.edu (K.J.M.B.).
† Department of Chemical and Biological Engineering, Northwestern University.
‡ Department of Chemistry, Northwestern University.
§ Polish Academy of Sciences.

10.1021/jp811473q CCC: $40.75
Published on Web 05/01/2009

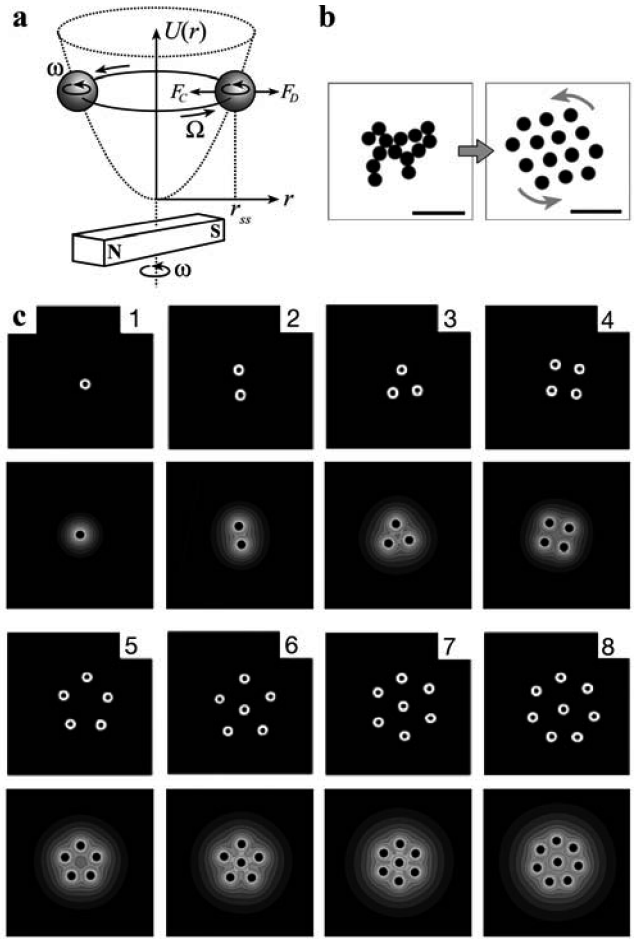

Figure 2. DySA of magnetic spinners. (a) Scheme of the experimental arrangement in which spinners rotate in viscous fluid with constant angular velocity ω equal to that of a rotating bar magnet. For finite fluid inertia ($Re \neq 0$), the vortices generated by the rotating particles induce a repulsive, dissipative force, F_D, which is balanced at steady state by conservative magnetic force, $F_C = -\nabla U$, due to the rotating magnet. The assembly of spinners (here, a pair) precesses around the magnet's axis of rotation with an angular velocity Ω, which depends on ω. (b) Experimental images of the magnetic particles with and without the applied rotating magnetic field. At equilibrium, the pieces float at a fluid−air interface and clump together via capillary forces (left). Introducing a nonequilibrium driving force (right)—here, the rotating magnetic field—the system "comes to life" creating a dynamic assembly maintained by vortex−vortex interactions. Scale bars = 5 mm. (c) Particle configurations for $n = 1$ to 8 spinners as observed in experiment (top) and simulation (bottom). The pictures from the simulations illustrate the magnitude of the local energy dissipation rate in the xy-plane as calculated by summation across the z-direction White and black colors correspond to regions of highest and lowest dissipation, respectively.

and others[20] have shown that the dynamic vortex−vortex forces between the "spinner" particles are repulsive and can be described by the concepts of low (but nonzero) Reynolds number (*Re*) hydrodynamics. The interplay between these forces and the confining magnetic potential acting on all rotating particles gives rise to the formation of open, two-dimensional arrays such as those shown in Figure 2b. Previously, we have studied the steady states of these dissipative assemblies based on the balance of forces acting on the particles.[17,18] Here, we approach this problem from a fundamentally different, thermodynamic perspective using the viscous energy dissipation rate.

Because, as we show, the DySA of "spinners" subject to an external potential does not obey Prigogine's minimal entropy production (MEP)[15] rule, it cannot be treated by the formalism of the near-equilibrium/linear regime of nonequilibrium thermodynamics. Consequently, we study this far-from-equilibrium DySA process by solving the governing Navier−Stokes equations and then calculating numerically the dissipation rates at various steady states. The results of these simulations reveal that despite finite *Re* and significant interparticle interactions, the excess dissipation rates are pairwise additive for steady states that correspond to the ordered particle assemblies. Importantly, imposition of any additional constraints on the system increases these dissipation rates and renders them nonadditive. If these results could be generalized to other dissipative, low-*Re* systems (notably, those based on colloidal or nanoscopic particles), they could provide a new thermodynamic rule governing the formation of ordered, nonequilibrium ensembles.

2. Experimental and Simulation Details

2a. Magnetohydrodynamic DySA.[16−19,21−23] The experimental DySA system we study comprises a collection of small, tens of micrometers to millimeter-sized magnetic particles (typically, polymer pieces loaded with magnetite) floating at a liquid−air interface and subject to a magnetic field produced by a rotating permanent magnet (cf. Figure 2). Under the influence of this magnet, all particles experience a centrosymmetric, conservative force F_C directed toward the magnet's axis of rotation and increasing in magnitude with the distance from this axis, r.[17] At the same time, the rotating field causes the particles to spin around their axes at an angular velocity, ω (typically, ~10 Hz) equal to that of the magnet. These rotations create vortices in the surrounding fluid and give rise to repulsive vortex−vortex forces, F_D, between the particles. Importantly, these interactions are dissipative such that they persist only as long as the particles are kept spinning. The competition between conservative and dissipative forces evolves the system into open-lattice, steady-state assemblies that slowly precess about the axis of the magnet with an angular velocity $\Omega \sim 0.01$ Hz.

2b. Simulations of the System's Dynamics. In the simulations, the system was treated as a collection of n neutrally buoyant spheres of radius a rotating with constant angular velocity, ω, in a viscous fluid. The motion of the fluid outside the spheres was governed by the Navier−Stokes equations for an incompressible, Newtonian fluid. Scaling times by ω^{-1}, lengths by a, velocities by $a\omega$, and pressure by $\mu\omega$, where μ is the dynamic viscosity, the dimensionless equations were written as $Re[\partial\vec{u}/\partial t + \vec{u}\cdot\nabla\vec{u}] = -\nabla p + \nabla^2\vec{u}$ and $\nabla\cdot\vec{u} = 0$, where $Re = \rho a^2\omega/\mu$ is the Reynolds number describing the relative magnitudes of inertial and viscous effects (in experiments, *Re* is ~0.01−1), and ρ is the fluid density. At the surface of the spheres, the velocity of the fluid was set equal to that of the solid surface (i.e., "no slip" condition); far from the spheres, the fluid velocity approached zero. The NS equations were solved numerically on a 128^3 grid with periodic boundary conditions using the so-called force coupling method (FCM), in which the solid spheres are approximated by locally distributed body forces acting on the fluid (cf. ref 20 for numerical details). This method has been validated extensively through comparison with experiments for various types of fluidic systems,[24,25] including the DySA spinners.[20]

The fluid motions induced by the rotating spheres gave rise to the vortex−vortex forces. Introducing the stress tensor, $\boldsymbol{\sigma} = -p\boldsymbol{\delta} + \boldsymbol{\tau}$, where $\boldsymbol{\delta}$ is the unit tensor and $\boldsymbol{\tau} = [\nabla\vec{u} + (\nabla\vec{u})^t]$ is the viscous stress tensor, the force acting on sphere i could be expressed as $\vec{F}_D^{(i)} = \int_{S^{(i)}} \vec{n}\cdot\boldsymbol{\sigma}\, dS^{(i)}$, where $\vec{n}$ is the unit normal directed out of the particle, and integration is carried out over the sphere's surface (note that all quantities are dimensionless:

stress tensors are scaled by $\mu\omega$ and forces by $\mu\omega a^2$). In addition, all particles experienced magnetic forces produced by the rotating magnet and directed toward the magnet's axis of rotation. As was shown previously,[17,18] these forces were well approximated by the gradient of a quadratic "confining" magnetic potential and could therefore be written as $\vec{F}_C = -\beta\vec{r}$, where $\vec{r}$ is the radial position vector. With these two forces, the dynamics of the particles are described by $m^{(i)}\, d\vec{V}^{(i)}/dt = \vec{F}_D^{(i)} + \vec{F}_C^{(i)}$, where $m^{(i)} = (4/3)\pi a^3\rho$ is the mass of particle i, and $\vec{V}^{(i)}$ is its velocity.

2c. Viscous Energy Dissipation. The rate of viscous energy dissipation for a given flow field and configuration of spinners was calculated using the viscous dissipation function[26] as $\varepsilon = \int_V \Phi\, dV$ in dimensionless units (dissipation scaled by $\mu a^3\omega^2$) where the integral is taken over the entire simulation domain. The viscous dissipation function (Φ) is related to the various spatial derivatives of the velocity, and for an incompressible fluid can be written as

$$\Phi = 2\left[\left(\frac{\partial u_x}{\partial x}\right)^2 + \left(\frac{\partial u_y}{\partial y}\right)^2 + \left(\frac{\partial u_z}{\partial z}\right)^2\right] + \left[\frac{\partial u_y}{\partial x} + \frac{\partial u_x}{\partial y}\right]^2 + \left[\frac{\partial u_z}{\partial y} + \frac{\partial u_y}{\partial z}\right]^2 + \left[\frac{\partial u_x}{\partial z} + \frac{\partial u_z}{\partial x}\right]^2 \quad (1)$$

3. Results and Discussion

First, we verified the accuracy of the simulations by comparing the value of ε_1 calculated numerically by FCM with the analytical result for an isolated sphere[27] $\varepsilon_1 = 8\pi(1 + o(Re))$ ($o(Re)$ is a correction for low Re; subscript "1" denotes one particle). The two results agreed to within 0.02%.

Next, we calculated the dissipation rates for various particle numbers, n (see configurations in Figure 2), for Reynolds numbers 0.1 to 1, and for various interparticle separations. We first discuss the case of two spinners, which illustrates the essential physical phenomena and allows for defining quantities used later in our analysis.

As two rotating particles are brought together from infinity, they begin to "feel" one another and move in response to the flow field created by the neighboring spinner. As the distance between the particle centers, d (scaled by the particle radius a), decreases, the local shear forces on the surface closest to that of the adjacent particle increase significantly due to flows generated by this particle. Consequently, the torque, T, required to maintain the constant angular velocity, ω, of the particles increases, and the energy dissipation rate increases steadily above its infinite-separation value, $2T_\infty$ (where, $T_\infty = 8\pi(1 + o(Re))$). We note that this behavior is at odds with the MEP rule since the magnetic potential confining the particles is conservative (i.e., not contributing to dissipation), and the spontaneously forming, two-spinner assembly does not correspond to the state of minimal energy dissipation/entropy production.

The contours shown for the two-particle system in Figure 2 illustrate that dissipation increases most in the "interaction region" between the spinners. To quantify the dissipation due to the hydrodynamic interaction between the spinners, we define an excess energy dissipation rate for the two particle system as the difference between the dissipation of an interacting pair and the dissipation of two isolated spinners

$$\Delta\varepsilon_2 = \varepsilon_2 - 2\varepsilon_1 \quad (2)$$

As shown in Figure 3, for a given Re, the excess dissipation rate increases rapidly with decreasing d (a situation corresponding to increasing the strength of the magnetic confinement). This behavior is seen for all values of the Reynolds numbers studied.

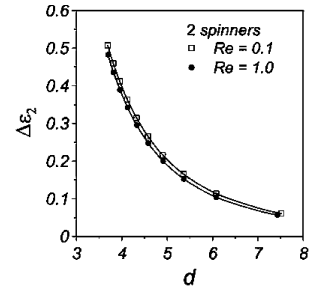

Figure 3. Excess energy dissipation rate for the spontaneously forming two-particle assemblies as a function of distance d between particle centers. As described in the text, the quantities are dimensionless with dissipation rate and distance scaled by $\mu a^3\omega^2$ and a, respectively. The results are largely independent of the Reynolds number in the range studied ($Re = 0.1, 1$).

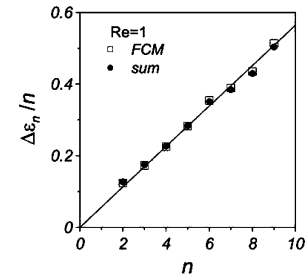

Figure 4. Excess energy dissipation rate per particle increases linearly with the number of particles in the assembly. The data points were calculated either directly via simulation ("FCM") or by pairwise summation of the two-particle result ("sum"). These two approaches agree to good approximation even at relatively large Reynolds numbers (here, $Re = 1$).

The concept of excess dissipation underlies one of the main findings of our study—namely, that for assemblies of $n > 2$ particles, the total dissipation ε_n (calculated by FCM) can be expressed as a sum of the dissipation rates of n individual/noninteracting spinners and that of pairwise, excess dissipation rates due to spinner−spinner interactions:

$$\varepsilon_n = n\varepsilon_1 + \Delta\varepsilon_n \qquad \text{where } \Delta\varepsilon_n = \sum_{i<j}^{n} \Delta\varepsilon_2(d_{ij}) \quad (3)$$

For example, the total dissipation of an assembly of $n = 3$ spinners is simply 3 times the dissipation of an individual spinner plus the excess dissipation term $\Delta\varepsilon_3 = \Delta\varepsilon_2(d_{12}) + \Delta\varepsilon_2(d_{13}) + \Delta\varepsilon_2(d_{23}) = 3\Delta\varepsilon_2(d)$ where the distances between the spinners are equal in the steady-state equilateral triangle configuration, $d_{12} = d_{13} = d_{23} = d$. In other words, the excess dissipation rates due to the interactions between the particles are pairwise additive. The linearity of the dependencies of $\Delta\varepsilon_n$ on n shown in Figure 4 illustrates that this conclusion holds for all n's studied and also for the entire range of Re values we considered.

We make two important comments about this result.

(i) Dissipation Additivity in the Stokes Limit. To better understand the origins of the above results, it is instructive to consider analytically the behavior of two and three spinners in the so-called Stokes limit (i.e., $Re = 0$). Due to the linearity of the governing equations, any linear superposition of constituent velocity fields satisfying the Stokes equations will also result in valid solutions to the Stokes equations. Furthermore, the dissipation function, Φ, of such a composite flow field (e.g., $\bar{u}$

$= \vec{u}_1 + \vec{u}_2 + \vec{u}_3$) can be expressed completely in terms of the dissipation function of the constituent fields, $\Phi(\vec{u}_i)$, plus pairwise contributions, $\Phi(\vec{u}_i + \vec{u}_j) - \Phi(\vec{u}_i) - \Phi(\vec{u}_j)$ (cf. Supporting Information for details). The absence of higher, many-body corrections derives from the explicit form of dissipation function (see eq 1) which comprises only quadratic terms of linear differential operators. Importantly, however, the above arguments *cannot* explain the origins of the observed dissipation additivity in any system of rigid particles, in particular, the DySA system described here.

The reason for this is that, even in the Stokes limit, simple addition of the flows due to the individual spinners—while satisfying the governing equations—cannot yield the overall flow as this superposition will fail to satisfy the boundary conditions at the surface of the spheres. In other words, a simple superposition will completely neglect the hydrodynamic interactions between the rotating particles. To account for these interactions and their effects on the energy dissipation rate, we applied the iterative perturbation scheme known as the method of reflections[28] to approximate the forces, torques, and dissipation rates for a system of rotating and translating particles (cf. Supporting Information for details). For the two-particle assemblies, the excess dissipation is approximated as

$$\Delta\varepsilon_2 = \pi\left[\left(\frac{2}{d}\right)^3 + O\left\{\left(\frac{2}{d}\right)^5\right\}\right] \quad \text{for } Re = 0 \tag{4}$$

where d is the distance between the two spinners, and this expression assumes that no forces are applied to the particles. Similarly, for three-particle assemblies, the excess dissipation in the Stokes limits is given by

$$\Delta\varepsilon_3 = 3\pi\left[\left(\frac{2}{d}\right)^3 + O\left\{\left(\frac{2}{d}\right)^5\right\}\right] \quad \text{for } Re = 0 \tag{5}$$

Thus, to fourth order (i.e., $O\{(2/d)^4\}$), we find that the excess dissipation rate for three spinners is exactly a pairwise summation of the two particle dissipation, $\Delta\varepsilon_3 = 3\Delta\varepsilon_2$.

Interestingly, the pairwise additivity of the excess dissipation rate does not originate from pairwise forces and torques between the particles. For example, in the three-particle assemblies there are nonnegligible three-body interactions that depend on the positions and velocities of all three particles (in general, three-body forces and torques are of order $O(d^{-1})$ and $O(d^{-2})$, respectively). In fact, the excess dissipation for three particles in the absence of three-body interactions is given by

$$\Delta\varepsilon_3^{(2)} = 3\pi\left[\left(\frac{2}{d}\right)^3 - \frac{3}{8}\left(\frac{2}{d}\right)^4 + O\left\{\left(\frac{2}{d}\right)^5\right\}\right] \neq 3\Delta\varepsilon_2 \tag{6}$$

It is only by the including three-body interactions, $\Delta\varepsilon_3^{(3)}$, that the excess dissipation rate becomes pairwise additive.

Although we consider only approximate solutions and a maximum of three spinners, these results in the Stokes limit agree very well with numerical simulations for finite *Re* and are therefore expected to hold for more particles and higher approximations. The major difference between the zero *Re* and finite *Re* assemblies is the absence of the repulsive vortex−vortex forces in the Stokes limit. For finite *Re*, however, these inertial forces are exactly balanced by the confining potential such that a "confined" system at finite *Re* is directly analogous to an unconstrained ("force-free") system in the Stokes limit. The effects of additional constraints are discussed in the next section.

Overall, we find that the excess dissipation rate is a pairwise additive quantity for naturally forming, dissipative assemblies of three or more particles and for $Re \leq 1$. This result is not a simple consequence of the linearity of the governing equations in the Stokes limit nor is it due to the absence of many-body interactions between the rotating particles. Instead, the motions and configurations of the assembling particles are exactly that which give rise to the surprising and counterintuitive result of pairwise dissipation additivity. So far, the above result has been demonstrated only for particles separated by distances larger than $d = 3.7$; for smaller d, both the numerical force coupling method and the analytical method of reflections become inaccurate. Testing the validity of this result at smaller separations will likely require the use of direct numerical simulations accounting explicitly for the rigid particle surfaces or alternative analytical approximations (e.g., the lubrication approximation).

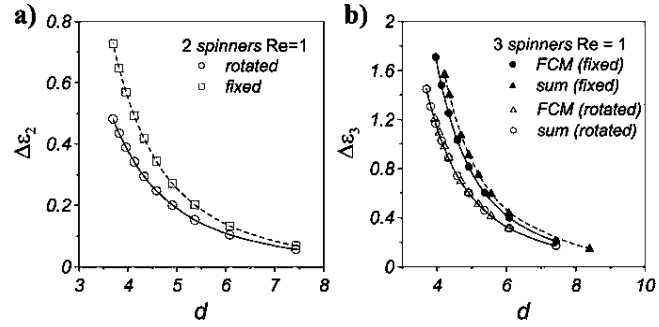

Figure 5. Excess energy dissipation rate as a function of the distance d between spinners as calculated by simulations. Here, the dissipation rate is smaller for the unconstrained rotating assemblies ("rotated", $\Omega > 0$) than for the constrained assemblies with fixed positions of the spinners ("fixed", $\Omega = 0$). This is illustrated for (a) two particles and for (b) three particles. In the three-particle assemblies, the dissipation was calculated directly ("FCM") or by pairwise summation of the two-particle result ("sum"). These two approaches agree in the unconstrained assemblies but not in the "fixed" particle arrangements.

(ii) Dissipation Additivity and Additional Constraints. Pairwise additivity of the excess dissipation rate is valid only in the naturally forming, steady states of the system. When any additional constraints are added, the additivity of excess dissipations does not hold. To show this, we performed simulations in which the rotating spinners were arranged in the polygonal patterns like the ones shown in Figure 2, but an externally applied force prevented the patterns from precessing (i.e., $\Omega = 0$). Figure 5a shows that for all particle separations, d, the dissipation for a pair of such "fixed" spinners is higher than the dissipation of a pair free to precess, $\varepsilon_2^{\text{fix}} > \varepsilon_2$. Moreover, Figure 5b shows that for a triangular configuration, $n = 3$, the excess dissipation of the fixed structures is no longer expressible by the sum of pairwise excess dissipations. This result extends to other n's studied, and in general, $\Delta\varepsilon_n^{\text{fix}} \neq \sum_{i<j}^{n} \Delta\varepsilon_2(d_{ij})$.

The effects of such constraints can be seen explicitly in the Stokes limit, for which accurate analytical approximations are possible. Specifically, the excess dissipation for two particles fixed in place but rotating about their own axes is given by

$$\Delta\varepsilon_2^{\text{fix}} = \pi\left[\left(\frac{2}{d}\right)^3 + \frac{3}{4}\left(\frac{2}{d}\right)^4 + O\left\{\left(\frac{2}{d}\right)^5\right\}\right] \tag{7}$$

Comparison with eq 4 shows clearly that $\varepsilon_2^{\text{fix}} > \varepsilon_2$. For three "fixed" particles, the excess dissipation is approximated as

$$\Delta\varepsilon_3^{\text{fix}} = 3\pi\left[\left(\frac{2}{d}\right)^3 + \frac{9}{8}\left(\frac{2}{d}\right)^4 + O\left\{\left(\frac{2}{d}\right)^5\right\}\right] \tag{8}$$

Unlike the unconstrained case for which $\Delta\varepsilon_3 = 3\Delta\varepsilon_2$, the excess dissipation is no longer pairwise additive upon addition of further constraints, e.g., $\Delta\varepsilon_3^{\text{fixed}} \neq 3\Delta\varepsilon_2^{\text{fixed}}$.

The above considerations lead us to the following conjecture: for small but finite *Re* ($Re \leq 1$), the addition of applied constraints to the particle motions can only act to increase the

total dissipation rate of a hydrodynamic system. This conjecture is readily verified analytically for the two-particle system in the Stokes limit. Specifically, for two rotating particles separated by a distance d, the steady-state configuration consists of particles precessing about a circular trajectory of radius $r = d/2$ with an angular precession velocity, $\Omega_{ss}(r)$. For this configuration, there are no net forces acting on the particles in the direction of their movement (for finite Re, however, there is a net repulsive force acting perpendicular to the direction of movement; this force is balanced by the confining force field), and the angular precession velocity may be expressed as $\Omega_{ss}(r) = f_1(r)/rf_2(r)$, where f_1 and f_2 are dimensionless force coefficients (as given by complex infinite series; cf. ref 29). Increasing or decreasing the precession velocity requires the application of an applied force, F, in the direction tangential to the particles' orbit. Below we show that this force can only act to increase the rate of viscous energy dissipation in the two-particle system.

At steady state, the dissipation rate is directly equal to the power delivered to the system by the rotation and translation of the solid particles, $\varepsilon = 2(T + Fr\Omega)$, where $T = 8\pi[g_1(r) - r\Omega g_2(r)]$ is the torque on each particle, $F = -6\pi[f_1(r) - r\Omega f_2(r)]$ is the force on each particle, and $g_1(r)$ and $g_2(r)$ are dimensionless couple coefficients (cf. Supporting Information and ref 29). Minimizing the total dissipation rate with respect to the angular precession velocity yields the following expression for the angular velocity of the minimum dissipation configuration, $\Omega_{min}(r) = [3f_1(r) + 4g_2(r)]/6rf_2(r)$. Quite remarkably, this expression is numerically identical (despite differences in the explicit functional form) to the above expression for $\Omega_{ss}(r)$, which was derived by setting the applied force to zero. Thus, from this example, we propose that the force-free configuration is exactly that which minimizes the viscous dissipation, and the addition of an applied forces acts only to increase the dissipation. Although our conjecture may only be proved analytically for the relatively simple example given above, it also appears to hold for small, finite Reynolds numbers and for more than two particles as evidenced by numerical simulation.

4. Conclusions

In sum, we have explored the nonequilbrium thermodynamics, namely, the viscous energy dissipation rate, of a prototypically magnetohydrodynamic DySA system. For this low Reynolds number fluidic system, we have found that the naturally forming steady-state configurations/flows may be characterized by three fundamentally different properties. The first is the well-established criterion of mechanical equilibrium that the steady-state configuration is that in which the forces and torques (fluidic or otherwise) acting on the particles are balanced. The second is that the rate of energy dissipation is minimal subject to the constraints of the confining magnetic potential. Finally and most intriguingly, the total dissipation of the n-particle system may be expressed as a sum of pairwise "interactions" derived from the analogous two-particle system. Each of these complementary descriptions provides a unique perspective through which to analyze the behaviors of "force-free" particles immersed in a viscous fluid, e.g., colloidal suspensions of rotating or nonrotating particles. While the first two have been explored in some detail, the concept of pairwise dissipation additivity is previously unreported and could provide a useful tool for the analysis of colloidal systems. For example, it could be used to calculate the apparent viscosity of a colloidal dispersion under shear using only the pairwise dissipation function, $\Delta\varepsilon_2(r)$, and the radial pair distribution function, $g(r)$. Current theoretical treatments of concentrated suspensions account only for pairwise interactions[30] and are therefore limited to the case of semidilute suspensions, in which many-body effects are negligible. Because the pairwise additivity of dissipation holds despite the presence of such many-body effects, it may provide a simpler approach toward addressing the behaviors of even concentrated colloidal suspensions.

Acknowledgment. We are grateful to Professor M. R. Maxey and Professor E. Climent for the code used in performing the simulations. Part of the calculations was performed at the Poznań Supercomputing and Networking Center (PCSS) in Poland.

Supporting Information Available: (1) Additivity of excess dissipation for additive flow fields; (2) Stokes limit: two and three particles by the method of reflections; and (3) detailed discussion of the minimum dissipation example (two spheres, $Re = 0$). This material is available free of charge via the Internet at http://pubs.acs.org.

References and Notes

(1) Whitesides, G. M.; Grzybowski, B. *Science* **2002**, *295*, 2418.
(2) Fialkowski, M.; Bishop, K. J. M.; Klajn, R.; Smoukov, S. K.; Campbell, C. J.; Grzybowski, B. A. *J. Phys. Chem. B* **2006**, *110*, 2482.
(3) Love, J. C.; Estroff, L. A.; Kriebel, J. K.; Nuzzo, R. G.; Whitesides, G. M. *Chem. Rev.* **2005**, *105*, 1103.
(4) Witt, D.; Klajn, R.; Barski, P.; Grzybowski, B. A. *Curr. Org. Chem.* **2004**, *8*, 1763.
(5) Kato, T. *Science* **2002**, *295*, 2414.
(6) Charra, F.; Cousty, J. *Phys. Rev. Lett.* **1998**, *80*, 1682.
(7) Eddaoudi, M.; Moler, D. B.; Li, H. L.; Chen, B. L.; Reineke, T. M.; O'Keeffe, M.; Yaghi, O. M. *Acc. Chem. Res.* **2001**, *34*, 319.
(8) Tanev, P. T.; Pinnavaia, T. J. *Science* **1995**, *267*, 865.
(9) Kalsin, A. M.; Fialkowski, M.; Paszewski, M.; Smoukov, S. K.; Bishop, K. J. M.; Grzybowski, B. A. *Science* **2006**, *312*, 420.
(10) Xia, Y. N.; Gates, B.; Yin, Y. D.; Lu, Y. *Adv. Mater.* **2000**, *12*, 693.
(11) Boncheva, M.; Ferrigno, R.; Bruzewicz, D. A.; Whitesides, G. M. *Angew. Chem., Int. Ed.* **2003**, *42*, 3368.
(12) Capito, R. M.; Azevedo, H. S.; Velichko, Y. S.; Mata, A.; Stupp, S. I. *Science* **2008**, *319*, 1812.
(13) Nicolis, G.; Prigogine, I. *Self-Organization in Nonequilibrium Systems: From Dissipative Structures to Order Through Fluctuations*; Wiley: New York, 1977.
(14) This refers to the so-called linear regime of nonequilibrium thermodynamics, in which the fluxes are linear functions of the various thermodynamic forces, and the assumption of local thermodynamic equilibrium remains valid.
(15) de Groot, S. R.; Mazur, P. *Nonequilibrium thermodynamics*; Dover Publications: New York, 1984.
(16) Grzybowski, B. A.; Stone, H. A.; Whitesides, G. M. *Nature (London)* **2000**, *405*, 1033.
(17) Grzybowski, B. A.; Jiang, X. Y.; Stone, H. A.; Whitesides, G. M. *Phys. Rev. E* **2001**, *64*, 011603.
(18) Grzybowski, B. A.; Stone, H. A.; Whitesides, G. M. *Proc. Natl. Acad. Sci. U.S.A.* **2002**, *99*, 4147.
(19) Grzybowski, B. A.; Whitesides, G. M. *J. Phys. Chem. B* **2001**, *105*, 8770.
(20) Climent, E.; Yeo, K.; Maxey, M. R.; Karniadakis, G. E. *J. Fluids Eng.—Trans. ASME* **2007**, *129*, 379.
(21) Grzybowski, B. A.; Whitesides, G. M. *J. Phys. Chem. B* **2002**, *106*, 1188.
(22) Grzybowski, B. A.; Whitesides, G. M. *J. Chem. Phys.* **2002**, *115*, 8571.
(23) Grzybowski, B. A.; Whitesides, G. M. *Science* **2002**, *296*, 718.
(24) Liu, D.; Maxey, M.; Karniadakis, G. E. *J. Microelectromech. Syst.* **2002**, *11*, 691.
(25) Lomholt, S.; Maxey, M. R. *J. Comput. Phys.* **2003**, *184*, 381.
(26) Deen, W. M. *Analysis of Transport Phenomena*; Oxford University Press: Oxford, UK, 1998.
(27) Rubinow, S. I.; Keller, J. B. *J. Fluid Mech.* **1961**, *11*, 447.
(28) Kim, S.; Karrila, S. J. *Microhydrodynamics: Principles and Selected Applications*; Dover: New York, 2005.
(29) Oneill, M. E. *Appl. Sci. Res.* **1970**, *21*, 452.
(30) Batchelor, G. K. *J. Fluid Mech.* **1977**, *83*, 97.
(31) Soh, S.; Bishop, K. J. M.; Grzybowski, B. A. *J. Phys. Chem. B* **2008**, *112*, 10848.

JP811473Q